2021 43rd Annual International Conference of the
IEEE Engineering in Medicine & Biology Society (EMBC)
Oct 31 - Nov 4, 2021. Virtual Conference

Predicting Driver Stress Levels with a Sensor-Equipped Steering Wheel and a Quality-Aware Heart Rate Measurement Algorithm

Raymundo Cassani[1], Atsushi Horai[2], Lucian A. Gheorghe[2], and Tiago H. Falk[1]
[1] Institut National de la Recherche Scientifique (INRS-EMT), University of Quebec, Montreal, Canada
[2] Nissan Research Center, Nissan Motors. Co., LTD, Kanagawa, Japan

***Abstract*— Unobtrusive monitoring of driver mental states has been regarded as an important element in improving the safety of existing transportation systems. While many solutions exist relying on camera-based systems for e.g., drowsiness detection, these can be sensitive to varying lighting conditions and to driver facial accessories, such as eye/sunglasses. In this work, we evaluate the use of physiological signals derived from sensors embedded directly into the steering wheel. In particular, we are interested in monitoring driver stress levels. To achieve this goal, we first propose a modulation spectral signal representation to reliably extract electrocardiogram (ECG) signals from the steering wheel sensors, thus allowing for heart rate and heart rate variability features to be computed. When input to a simple logistic regression classifier, we show that up to 72% accuracy can be achieved when discriminating between stressful and non-stressful driving conditions. In particular, the proposed modulation spectral signal representation allows for direct quality assessment of the obtained heart rate information, thus can provide additional intelligence to autonomous driver monitoring systems.**

I. INTRODUCTION

The National Highway Traffic Safety Administration reported that in 2017 alone there were around 6.5 million car crashes in the United States [1], almost half of which were related to the mental state of the driver [2]. Accurate measurement of mental states such as, workload, fatigue, drowsiness, and stress, can improve the interaction with adaptable intelligent systems [3], and in the case of intelligent vehicles, can lead to improved road safety [4].

Automated driver status monitoring systems are often based on cameras focusing on eye gaze, eye movement, and pupillometry information. Such systems, however, may compromise driver privacy, and can be sensitive to lighting changes and to facial accessories used by drivers, such as eye or sunglasses [5]. To overcome this, exploratory work has been conducted with vehicle add-on devices, such as electroencephalogram (EEG) and near-infrared spectroscopy (NIRS) headsets [6], or sensors to measure electrocardiogram (ECG), electrodermal activity (EDA), photoplethysmogram (PPG) and breathing rate information [7], [8], [9], [10], [11].

Unfortunately, not all physiological signals can be measured in a non-intrusive manner and relying on drivers to wear an additional device, such as headbands, chestbands and/or smartwatches is unrealistic in practice. As such, sensors embedded directly into the vehicle have gained interest lately, with sensors being placed in steering wheels and car seats being the most popular [5]. Seat-based sensors, however, have shown to be sensitive to factors such as driving position and driver size [12]. In turn, steering wheel based sensors are sensitive to changes in the electrical contact between the sensors and driver hands, as the wheel position changes. Such artifacts can severely compromise the usability of the obtained ECG signal.

Accurate measurement of ECG from the steering wheel is pivotal to reliably estimate hearth rate (HR) and heart rate variability (HRV) [13], [14]. Within the context of driving, HRV features have found to be useful in the estimation of driver stress [15], mental workload [16], drowsiness and fatigue [17]. Here, we propose a new algorithm based on a modulation spectral signal representation to obtain a reliable estimate of the steering wheel ECG (ECG_{sw}). To validate our estimates, we first gauge the effectiveness of the proposed method against HR from a portable ECG device (henceforth termed "ground truth" ECG, ECG_{gt}). Once the estimated HR measures are validated, traditional HRV measures are computed and serve as input to stress detection classifiers. Results are reported per driver and across all drivers. Additionally, the modulation spectral signal representation provides a direct quality measure of the steering wheel ECG, thus can be used as context for machine learning algorithms. The remainder of this article is organized as follows. In Section II we describe the experimental protocol, and present the methods used for the signal processing, feature extraction and stress-level classification. In Section III, the experimental results are presented alongside a discussion on them. Finally, conclusions are presented in Section IV.

II. METHODS AND MATERIALS

A. Experimental protocol

Four participants were required to drive in a car simulator during two conditions: *no-stress* and *stress*. Each condition consisted of two laps of a winding circuit road (5 km). In the *no-stress* condition, the participants were only required to keep their lane. In the *stress* condition, besides keeping their lane, the participants were also required to follow a car as close as possible without hitting it. In both conditions, the participant had full control of the car (i.e., accelerator, break, and steering wheel). Each condition had a duration of approximately 9 minutes.

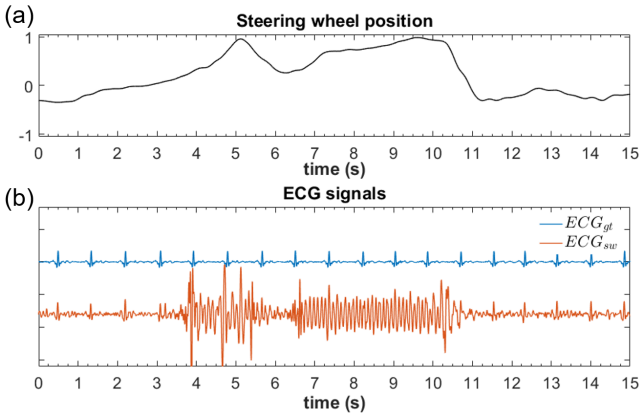

Fig. 1. Example of artifacts due to steering wheel maneuvering. (a) Steering wheel position. (b) ECG signals, ECG_{gt} (blue) and ECG_{sw} (red).

B. Signal acquisition

During the driving tasks, for each participant, seven ECG signals were acquired from electrodes embedded in the steering wheel [14]. In this work we made use of the ECG_5 signal in the wheel (see details in [14]), henceforth referred to as ECG_{sw}. Simultaneously, ground truth ECG (ECG_{gt}) was acquired from disposable Ag-AgCl electrodes placed on the right clavicle and the lowest left rib. Both ECG signals were acquired with a multimodal biosignal amplifier (Bitbrain Technologies, Spain). In addition of the physiological signals, time-aligned car status and position in the winding circuit road were acquired from the car simulator.

C. Subjective metrics

After each driving condition, the participants answered the NASA Task Load Index (NASA-TLX) questionnaire, [18], and provided a score between 0 and 100 about their sleepiness during the driving condition. From the NASA-TLX, the adaptive weighted workload (AWWL) was calculated, as described in [19]. A value for arousal was calculated as 100 minus the reported sleepiness score. As result, the AWWL and arousal scores are in the 0-100 range.

D. Signal processing, HR estimation, and HRV features

Both ECG_{gt} and ECG_{sw} signals were bandpass filtered with a zero-phase FIR filter with a bandwidth from 5 to 30 Hz to remove baseline wandering and enhance the QRS complex waveform. We first used the Pan-Tomkins algorithm (PT) [20] to find the R-peak locations in ECG_{gt} and ECG_{sw}. From these locations, the RR intervals (RRs) were derived and the instantaneous HR was computed. The PT algorithm, however, was shown to be very sensitive to the large artifacts present in the ECG_{sw} signal resultant from the unsteady contact between the hands and the electrodes on the steering wheel during maneuvers. As an example, Fig. 1a shows the steering wheel position during a maneuver and subplot b shows the $ECGF_{gt}$ (blue) and the corresponding ECG_{sw} (red) signals. As can be seen, the artifacts are numerous during maneuvers.

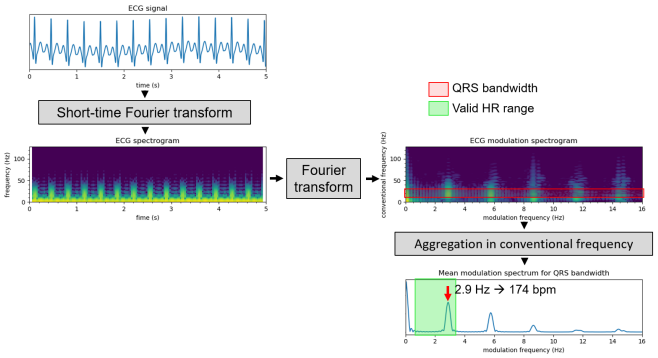

Fig. 2. Processing steps involved in the computation of the modulation spectrogram and, ultimately, of the HR.

To address this issue, we propose a HR measurement algorithm based on the modulation spectrogram (MS) representation. This was shown to be more robust to artifacts in [14]. For a time-domain signal, $x(t)$, its spectrogram, $X(t, f)$, is a complex-valued spectrotemporal representation that provides time-dependent information on amplitude and phase changes over time for different frequency components. The spectrogram is commonly computed with the short-time Fourier transform (STFT). The modulation spectrogram, $X(f, f_{mod})$, is the natural extension of the spectrogram, as it characterizes the periodicities in the amplitude changes for each (conventional) frequency component in the spectrogram. This is achieved by applying a time-to-frequency transform across the time dimension of the spectrogram. As such, the MS provides a representation of second-order periodicities, or modulation frequencies. These modulation frequency components are sometimes referred to as "hidden periodicities" as they are not observed in the spectrum or the signal, nor in its spectrogram [21]. The MS is computed as:

$$X(f, f_{mod}) = \mathcal{F}_t \left\{ |X(t, f)| \right\}, \tag{1}$$

where $\mathcal{F}_t\{\cdot\}$ is the Fourier transform operator that is applied to the time dimension of the spectrogram $X(t, f)$. Thus, the MS is a 2D representation of conventional frequency vs. modulation frequency. The relevance of the MS for processing ECG relies on the periodicities of the ECG signal. The HR is derived by finding the main modulation frequency for the conventional frequency components that correspond to the QRS complex. This main modulation frequency is found by averaging the MS modulus across the conventional frequency axis for the spectral components of the QRS complex. This process is depicted by Fig. 2. ECG signals were analyzed in 10-s segments with 5-s overlap, and the spectrogram was computed with the STFT using windows of 0.125 s with an overlap of 75%. In addition, the MS has shown to be useful as a quality metric. In [22], an ECG quality index termed *MSQI* was proposed and consists of the ratio of ECG energy to non-ECG energy in the modulation domain. It was shown that an *MSQI* > 0.5 indicates acceptable ECG quality. The interested reader is referred to [22] for more details about the quality index. Here, we propose an improvement to the HR measurement algorithm in [14] and use the *MSQI* as a parameter to gauge the reliability

of the estimated HR. If HR values are not acceptable, those stored in a 5-sample buffer are used. Sudden changes in HR measures are indicative of artifacts and are filtered out. This algorithm is described in Algorithm 1.

Algorithm 1: Filter HR values

input : new HR value: HR_{in},
new MSQI: $MSQI_{in}$
HR values in buffer: HR_{buf}
output: valid HR value, HR_{out}

$RR_{in} \leftarrow 60/HR_{in}$
$RR_{buf} \leftarrow 60/HR_{buf}$
if $|RR_{in} - \overline{RR_{buf}}| > \overline{RR_{buf}} \times 0.2$ **then**
  if $(2 \times RR_{in}) \approx RR_{buf}$ **then**
    $RR_{in} \leftarrow RR_{in} \times 2$
    $RR_{out} \leftarrow RR_{in}$
  else
    $RR_{out} \leftarrow \overline{RR_{buf}}$
    if $MSQI_{in} < 0.5$ **then**
      $RR_{in} \leftarrow \overline{RR_{buf}}$
    end
  end
else
  $RR_{out} \leftarrow RR_{in}$
end
Update RR_{buf} by adding RR_{in}
$HR_{out} \leftarrow 60/RR_{out}$
$HR_{buf} \leftarrow 60/RR_{buf}$

To gauge the effectiveness of the proposed MS-based method to estimate HR, the ground truth HR values obtained from the chest ECG were used. More specifically, since the chest ECG was artifact free, the average RR curve derived from the ECG_{gt} signal and the classic PT algorithm was used, for each 10-s segment. This RR values were used to calculate the HR time series that is referred to as avg_HR_{gt}. For comparison purposes, the avg_HR_{sw} was also derived from the ECG_{sw} signal and the PT algorithm; this is to be used as a benchmark. In turn, the MS-based HR time series that were obtained by the proposed algorithms from ECG_{gt} and ECG_{sw} are termed ms_HR_{gt} and ms_HR_{sw}, respectively. As a result, for each participant under each driving condition there are four HR time series, namely: avg_HR_{gt}, avg_HR_{sw}, ms_HR_{gt}, and ms_HR_{sw}, each sampled every 5 seconds (or at 0.2 Hz).

Finally, HRV features were computed from the HR time series. Although HRV features are often computed from the instantaneous HR time series [13], recently, it has been shown that time-domain HRV features computed from low temporal resolution HR time series can provide insightful information as well [23]. A total of seven time-domain HRV features were computed: mean RR, std. of RR (SDNN), coefficient of variation of RR (CVRR), percentage of RR differences larger than 50 ms (pNN50), mean of the first RR difference, std. of absolute first RR difference (std. 1diff. RR), root mean square of first RR difference (RMSDD), and mean absolute first difference of normalized RR.

E. Subjective ratings and stress classification

The changes in AWWL and arousal w.r.t the driving conditions were analyzed, as well as their correlation with the stress levels. With the computed HRV features, we trained a logistic regression classifier (one for each participant and one for all the participants) to perform binary stress classification.

TABLE I
RMSE VALUES FOR HR ESTIMATION.

Part.	Cond.	avg_HR_{sw} vs. avg_HR_{gt}	ms_HR_{gt} vs. avg_HR_{gt}	ms_HR_{sw} vs. avg_HR_{gt}	ms_HR_{sw} vs. ms_HR_{gt}
#1	no-stress	52.796	0.054	0.017	0.037
	stress	66.478	0.094	1.930	2.023
#2	no-stress	0.147	0.215	0.140	0.076
	stress	1.966	1.246	0.185	1.430
#3	no-stress	0.003	0.023	0.023	0.000
	stress	0.013	0.037	0.051	0.014
#4	no-stress	19.200	0.025	0.122	0.097
	stress	18.410	0.086	0.121	0.207
All	no-stress	18.036	0.079	0.075	0.052
	stress	24.865	0.092	0.064	0.043
All	**all**	**19.876**	**0.222**	**0.323**	**0.485**

The classifiers were evaluated 100 times under a 5-fold cross-validation approach. For each classifier the 3 most relevant features were identified by the magnitude of their weights.

III. EXPERIMENTAL RESULTS AND DISCUSSION

A. HR estimation and ECG signal quality

To evaluate the proposed method, we computed the root-mean square error (RMSE) between avg_HR_{gt} (i.e., true HR measures) and the two proposed measures (ms_HR_{gt} and ms_HR_{sw}), as well as the benchmark based on the classical PT algorithm avg_HR_{sw}. Also, RMSE was computed between ms_HR_{gt} and ms_HR_{sw} to verify the artifact-robustness of the proposed method. RMSE was computed for each participant and condition, and are reported in Table I. The largest RMSE occurred between the avg_HR_{sw} and avg_HR_{gt} curves, thus corroborating the negative impact that hand-movement artifacts have on the estimation of HR when classic peak detection algorithms are used. This was particularly true for participants #1 and #4. On the other hand, the low RMSE obtained when the proposed method was used, corroborating that the MS approach reduces the negative effects of artifacts in HR estimation. This was true when compared to the ground truth ECG processed with the proposed and classic methods.

As expected, on average the ECG_{sw} signal presented lower *MSQI* values (0.63 ± 0.18), than the ECG_{gt} signal (0.87 ± 0.07). In both ECG signals, there was not significant difference in the *MSQI* values for the stress and no-stress conditions. To evaluate the changes in the ECG_{sw} signal quality across the road circuit, we normalized the MSQI values for each participant-condition pair, and aggregate them across participants, conditions and loops. The normalized MSQI values (nMSQIs) consisted in the obtained MSQIs scaled by the average MSQI for a given participant-condition pair. As a result, an overall quality was obtained for the entire circuit, this is depicted in Figure 3. As can be seen, the lowest quality is achieved during maneuvers. This information can be used in the future as real-time contextual cues for automated systems.

B. Analysis of subjective metrics and stress classification

All participants reported higher arousal scores under the stress condition, this increment was on average 35.6 ± 25. For AWWL, 3 participants reported higher values during the stress condition, the average change was 15.1 ± 21.5. Pearson correlation between AWWL and arousal resulted in negative

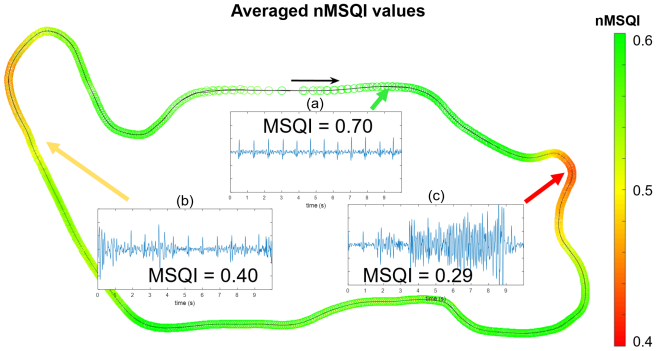

Fig. 3. Averaged nMSQI values across participants, conditions and loops, for ECG_{sw} signal. Subplots (a), (b) and (c) show 10-s segments of ECG_{sw} signal with good, medium and bad signal quality respectively.

TABLE II

ACCURACY AND TOP-3 FEATURES FOR STRESS CLASSIFICATION.

	Part. #1	**Part. #2**	**Part. #3**	**Part. #4**	**All**
Acc. %	88.0	65.8	60.7	59.4	**72.3**
(std.)	(4.5)	(8.0)	(9.5)	(9.2)	**(3.7)**
Feature ranking					
top-1	CVRR	CVRR	SDNN	SDNN	**CVRR**
top-2	SDNN	SDNN	CVRR	CVRR	**SDNN**
top-3	std. 1diff. RR	RMSDD	mean RR	mean RR	**RMSDD**

correlations -0.57 and -0.16 for no-stress and stress condition. As ms_HR_{sw} is a good estimate of the ground truth HR time series (according the results in Section III-A), HRV features were computed from the ms_HR_{sw} time series, and used for the binary classification task. Table II presents the per-participant and across-participant accuracies, as well as top-3 features. As can be seen, participant-wise accuracies ranged from 88%to 59%, and the classifier trained with all-participants data had an accuracy of 72%. In turn, CVRR and SDNN features appeared as the top-2 features across all classifiers. This relationship between HR features and stress is in line with similar studies that used chestbands to acquire the ECG signal [8], [9], [10], [11].

IV. CONCLUSIONS

In this work, we evaluated the use ECG signal acquired with sensors embedded on the steering wheel to discriminate between non-stressful and stressful driving conditions. First, we proposed a new quality-aware HR measurement algorithm based on a modulation spectrogram representation. The proposed method is robust to artifacts generated during maneuvers and achieved small errors relative to ground truth HR measures from chest ECG. HRV measures derived from the proposed method were used to estimate driver stress states and achieved an average accuracy of 72% across all participants. Future work will explore: *(i)* ECG quality metrics as context for machine learning algorithms, and (ii) the addition of other non-intrusive signals such EDA.

REFERENCES

[1] National Highway Traffic Safety Administration, "Summary of Motor Vehicle Crashes 2017," https://crashstats.nhtsa.dot.gov/Api/Public/ViewPublication/812794, 2019, [Online; accessed December 2020].

[2] D. L. Hendricks, M. Freedman, J. C. Fell *et al.*, "The relative frequency of unsafe driving acts in serious traffic crashes," National Highway Traffic Safety Administration, Tech. Rep., 2001.

[3] R. W. Picard, *Affective computing*. MIT press, 2000.

[4] L. Fridman, "Human-centered autonomous vehicle systems: Principles of effective shared autonomy," *CoRR*, vol. abs/1810.01835, 2018. [Online]. Available: https://arxiv.org/abs/1810.01835

[5] Y. Choi, S. I. Han, S.-H. Kong, and H. Ko, "Driver Status Monitoring Systems for Smart Vehicles Using Physiological Sensors: A safety enhancement system from automobile manufacturers," *IEEE Signal Processing Magazine*, vol. 33, no. 6, pp. 22–34, Nov. 2016.

[6] M.-A. Moinnereau, S. Karimian-Azari, T. Sakuma, H. Boutani, L. Gheorghe, and T. H. Falk, "Eeg artifact removal for improved automated lane change detection while driving," in *2018 IEEE International SMC Conference*. IEEE, 2018, pp. 1076–1080.

[7] R. L. Charles and J. Nixon, "Measuring mental workload using physiological measures: A systematic review," *Applied Ergonomics*, vol. 74, pp. 221–232, Jan. 2019.

[8] J. Healey and R. Picard, "Detecting Stress During Real-World Driving Tasks Using Physiological Sensors," *IEEE Transactions on Intelligent Transportation Systems*, vol. 6, no. 2, pp. 156–166, Jun. 2005.

[9] A. S. Le, H. Aoki, F. Murase, and K. Ishida, "A Novel Method for Classifying Driver Mental Workload Under Naturalistic Conditions With Information From Near-Infrared Spectroscopy," *Frontiers in Human Neuroscience*, vol. 12, p. 431, Oct. 2018.

[10] M. Antoun, D. Ding, E. E. Bohn-Goldbaum, S. Michael, and K. M. Edwards, "Driving in an urban environment, the stress response and effects of exercise," *Ergonomics*, vol. 61, no. 9, pp. 1273–1281, Sep. 2018.

[11] P. Zontone, A. Affanni, R. Bernardini, L. Del Linz, A. Piras, and R. Rinaldo, "Stress Evaluation in Simulated Autonomous and Manual Driving through the Analysis of Skin Potential Response and Electrocardiogram Signals," *Sensors*, vol. 20, no. 9, p. 2494, Apr. 2020.

[12] T. Matsuda and M. Makikawa, "ECG monitoring of a car driver using capacitively-coupled electrodes," in *2008 30th Annual International Conference of the IEEE Engineering in Medicine and Biology Society*. Vancouver, BC: IEEE, Aug. 2008, pp. 1315–1318.

[13] Electrophysiology, Task Force of the European Society of Cardiology the North American Society of Pacing, "Heart Rate Variability," *Circulation*, vol. 93, no. 5, pp. 1043–1065, Mar. 1996.

[14] R. Cassani, T. H. Falk, A. Horai, and L. A. Gheorghe, "Evaluating the Measurement of Driver Heart and Breathing Rates from a Sensor-Equipped Steering Wheel using Spectrotemporal Signal Processing," in *2019 IEEE Intelligent Transportation Systems Conference (ITSC)*. Auckland, New Zealand: IEEE, Oct. 2019, pp. 2843–2847.

[15] A. Lanata, G. Valenza, A. Greco, C. Gentili, R. Bartolozzi, F. Bucchi, F. Frendo, and E. P. Scilingo, "How the Autonomic Nervous System and Driving Style Change With Incremental Stressing Conditions During Simulated Driving," *IEEE Transactions on Intelligent Transportation Systems*, vol. 16, no. 3, pp. 1505–1517, Jun. 2015.

[16] B. Eilebrecht, S. Wolter, J. Lem, H. Lindner, R. Vogt, M. Walter, and S. Leonhardt, "The relevance of HRV parameters for driver workload detection in real world driving," in *2012 Computing in Cardiology*, Sep. 2012, pp. 409–412.

[17] J. Vicente, P. Laguna, A. Bartra, and R. Bailón, "Drowsiness detection using heart rate variability," *Medical & Biological Engineering & Computing*, vol. 54, no. 6, pp. 927–937, Jun. 2016.

[18] S. G. Hart and L. E. Staveland, "Development of NASA-TLX (Task Load Index): Results of Empirical and Theoretical Research," in *Advances in Psychology*. Elsevier, 1988, vol. 52, pp. 139–183.

[19] S. Miyake and M. Kumashiro, "Subjective mental workload assessment technique," *The Japanese journal of ergonomics*, vol. 29, no. 6, pp. 399–408, 1993.

[20] J. Pan and W. J. Tompkins, "A real-time QRS detection algorithm," *IEEE transactions on biomedical engineering*, no. 3, pp. 230–236, 1985.

[21] R. Cassani and T. H. Falk, "Spectrotemporal Modeling of Biomedical Signals: Theoretical Foundation and Applications," in *Reference Module in Biomedical Sciences*. Elsevier, 2018.

[22] D. P. Tobon V., T. H. Falk, and M. Maier, "MS-QI: A Modulation Spectrum-Based ECG Quality Index for Telehealth Applications," *IEEE Transactions on Biomedical Engineering*, vol. 63, no. 8, pp. 1613–1622, Aug. 2016.

[23] A. Tiwari, R. Cassani, S. Narayanan, and T. H. Falk, "A Comparative Study of Stress and Anxiety Estimation in Ecological Settings Using a Smart-shirt and a Smart-bracelet," in *2019 41st Annual International Conference of the IEEE Engineering in Medicine and Biology Society (EMBC)*. Berlin, Germany: IEEE, Jul. 2019, pp. 2213–2216.